Journal of Materials Chemistry B

Accepted Manuscript

ROYAL SOCIETY OF CHEMISTRY

www.rsc.org/materialsB

Journal Name

RSCPublishing

ARTICLE

Structural impact of graft and block copolymers based on poly(*N*-vinylpyrrolidone) and poly(2-dimethylaminoethyl methacrylate) in gene delivery

onCite this: DOI: 10.1039/x0xx00000x

Received 00th January 2012,
Accepted 00th January 2012

DOI: 10.1039/x0xx00000x

www.rsc.org/

Xiang Zheng,†[ad] Tingbin Zhang,†[ad] Xiaoyan Song,*[c] Ling Zhang,[a] Chunqiu Zhang,[b] Shubin Jin,[b] Jinfeng Xing*[ad] and Xing-Jie Liang*[b]

Cationic polymers (polycations) are promising gene vectors that are conveniently to be synthesized and easily to be modified. In order to study the relationship between structures and properties of the polycations in gene delivery, the graft copolymer named poly(*N*-vinylpyrrolidone)-*g*-poly(2-dimethylaminoethyl methacrylate) (PVP-*g*-PDMAEMA, *i.e.* PgP) and block copolymer named PVP-*b*-PDMAEMA (PbP) with equal molecular weight of PDMAEMA and PVP were prepared by two advanced living radical polymerizations including atom transfer radical polymerization (ATRP) and reversible addition-fragmentation chain transfer (RAFT) technique. Compared with PbP, PgP could condense pDNA more effectively into polyplexes with smaller size, higher zeta potential and better stability. The transfection efficiency of PgP at low N/P ratio of 4:1 was not only higher than that of PbP, but also much higher than that of commercial available PEI as the gold standard of polycations and Lipofectamine. In addition, both PgP and PbP had less BSA absorption compared with PEI, indicating that the PVP could resist BSA absorption. In order to understand the mechanism behind the high transfection efficiency of PgP, cellular uptake and endosomal escape of PgP/pDNA and PbP/pDNA polyplexes were investigated. The results demonstrated that the improvement of the transfection efficiency of PgP originated from the promotion of the cellular uptake and endosome/lysosome escape. This study will provide useful information on designing effective non-viral vectors for gene delivery.

Introduction

Gene therapy has attracted much attention for its promising applications in the treatment of inherited and acquired diseases. The principle of gene therapy is that therapeutic genes are delivered into patient's host cells to produce or silence functional proteins to cure diseases.[1-4] The key factor for successful application of gene therapy is the gene vector with high transfection efficiency and low cytotoxicity.[5] Viral vectors generally have high transfection efficiency, but their clinical applications have been limited due to the safety concerns such as possible mutagenicity and severe immune response.[6] For their alternatives, non-viral vectors, especially polycations, such as polyethyleneimine (PEI),[7, 8] PDMAEMA,[9-11] poly(L-lysine) (PLL)[12, 13] and polyamidoamine (PAMAM)[14, 15] have achieved intense investigation due to their advantages, *e.g.* can be synthesized conveniently, modified easily, and has low immunogenicity.[16-19]

Among those polycations, PDMAEMA has shown great potential to construct perfect vector because of its versatile synthetic methods using ATRP or RAFT.[20-23] The graft copolymer and block copolymer based on PDMAEMA have been widely investigated in gene delivery.[24-28] Wang *et al.* reported the PDMAEMA grafted dextran based on polysaccharides (DPDS) by ATRP for gene delivery, which exhibited much lower cytotoxicity and much higher transfection efficiency than PDMAEMA and PEI in HEK 293 and L929 cells.[26] Guo *et al.* synthesized a temperature sensitive poly(ε-caprolactone)-*g*-poly(2-dimethylaminoethyl methacrylate) (PCL-*g*-PDMAEMA), which showed comparable transfection efficiency to Lipofectamine with obvious cytotoxicity when the N/P ratio was beyond 10 in 293T cells.[29] Qiao *et al.* synthesized the mPEG-*b*-PDMAEMA by ATRP to reduce the cytotoxicity of PDMAEMA. Although the cytotoxicity of mPEG-*b*-PDMAEMA was dramatically

reduced, the transfection efficiency was also decreased.[25] In order to improve the transfection efficiency and reduce the cytotoxicity of the polycations at the same time, Lin *et al.* synthesized PEG-*a*-PDMAEMA using a cyclic ortho ester linkage by ATRP. Although the transfection efficiency of PEG-*a*-PDMAEMA was higher than PDMAEMA at pH 5.0 and the cytotoxicity was also reduced, the transfection efficiency was much lower than that of PDMAEMA at pH 7.4 in 293T cells.[28] So far, the characteristics of graft copolymer and block copolymer based on PDMAEMA in pDNA compaction, polyplexes stability, cytotoxicity, transfection efficiency, internalization and intracellular distribution of polyplexes were not systematically investigated.

In this work, PgP and PbP with equal PDMAEMA segments were prepared via the living radical polymerization of ATRP and RAFT, respectively.[21-23] PDMAEMA with pendant tertiary amine groups can facilitate the endosomal escape of the polyplexes. PVP can shield the excess positive charge of PDMAEMA to reduce the cytotoxicity without sacrificing gene transfection efficiency of the polyplexes due to their synergistic role in gene delivery.[30, 31] The properties of PgP and PbP in pDNA encapsulation (Scheme 1) and gene delivery were systematically investigated *in vitro*, which could provide useful information for designing effective gene vectors in the future.

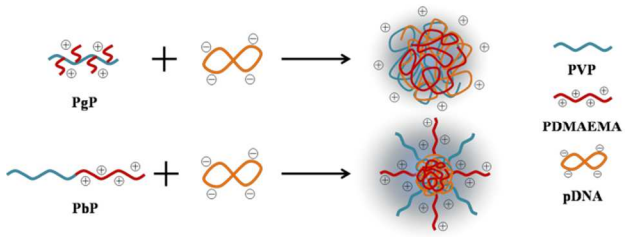

Scheme 1 The formation of PgP/pDNA and PbP/pDNA polyplexes.

Experimental

Materials

N-vinylpyrrolidone (Aldrich, 99%) was purified by distillation under reduced pressure to get rid of the inhibitor. 2-bromine ethyl propionate and potassium ethyl xanthate were purchased from Aladdin company. 2,2'-bipyridine (bPy) was purchased from Beijing Shiying Reagent Manufactory. CuBr was prepared in our laboratory and purified according to literature.[32] *N*-bromosuccinimide (NBS) and ethyl ether were purchased from Jiangtian Chemical Technology Co., Ltd (Tianjin, China). 2-dimethylaminoethyl methacrylate (DMAEMA, 97%) was purchased from Alfa Aesar. 2,2-Azobis(2-methylpropionitrile) (AIBN, Molecular) was recrystallized from methanol and stored at 4 °C in the dark. Dimethylformamide (DMF) was dried over anhydrous $CaCl_2$ and distilled under ultrahigh nitrogen before used. All other chemicals and solvents were analytical grade and used as received unless otherwise stated.

High Glucose dulbecco's modified eagle medium (H-DMEM), Opti-MEM I Reduced serum Medium (Opti-MEM), fetal bovine serum (FBS) and Penicillin-Streptomycin Solution were purchased from Gibco. Lipofectamine was obtained from Lianxing Corporation (Tianjin, China). Phosphate-buffered saline (PBS, pH 7.4) was purchased from Invitrogen Corporation (Carlsbad, CA). Ethidium bromide, dimethyl sulfoxide (DMSO) and 3-[4, 5-dimethylthiazol-2-yl]-2, 5-diphenyltetrazolium bromide (MTT) were purchased from Sigma-Aldrich (St Louis, Mo, USA). Agarose was purchased from GEN TECH (Hong Kong, China). EGFP-N1 plasmid (4700 bp) was extracted from escherichia coli according to the introduction procedure of plasmid extraction kit. Plasmid extraction kit was purchased from TIANGEN. Cy5-Oligo DNA was purchased from Sangon Biotech Co. Ltd (Shanghai, China).

Preparation of PgP

Macro chain transfer agent (CTA) was synthesized according to the reference.[33] 2-bromine ethyl propionate (1.7 mL, 16 mmol) and potassium ethyl xanthate (1.6 g, 10 mmol) were dissolved in 10 mL of absolute ethanol, respectively. The former was added into the latter drop by drop before stirring for 20 h at room temperature (25 °C), then the white precipitate was removed by filtration. The product was purified by column chromatography using petroleum ether/ethyl acetate (95:5 v/v) as the eluent. Light yellow oil S-(2-ethyl propionate)-O-ethyl xanthate (CTA) was obtained (50% yield).

To prepare PVP-Br, PVP-CTA was first synthesized by RAFT using CTA as initiator. In brief, NVP (2.68 mL, 25 mmol), AIBN (0.02 g, 0.1 mmol) and CTA (0.125 mL, 0.5 mmol) were dissolved in anhydrous DMF (1 mL) before deoxygenated and pumped by nitrogen sparging for 30 min. [22, 34] After stirring at 60 °C for 6 h, PVP-CTA was purified by repeating the process of dissolution in dichloromethane and precipitation in diethyl ether and dried under vacuum. Then, PVP-CTA (1.2 g, 0.2 mmol) was dissolved in deionized water (20 mL). The bromination reaction was carried out by adding CCl_4 (50 mL), NBS (3.2 g, 18 mmol) and AIBN (42 mg, 0.24 mmol) at 90 °C before stirring for 30 h. Then the reaction solution was purified by rotary evaporation, dialysis and freeze-drying to obtain PVP-Br, the initiator afterwards.

PVP-Br (0.16 g, 0.03 mmol) was dissolved in dry DMF (2 mL) in a 25 mL Schlenk tube, and then bPy (16.4 mg, 0.11 mmol), DMAEMA (2.52 mL, 15 mmol) and CuBr (7.85 mg, 0.055 mmol) were added to the tube under a dry nitrogen atmosphere.[35] The solution was stirred at 40 °C for 22 h. PgP was obtained after dialysis and freeze-drying (Scheme 2A).

Preparation of PbP

The chain transfer agent PVP-CTA was synthesized as described above. Then, PVP-CTA (1.8 g, 0.3 mmol), DMAEMA (2.52 mL, 15 mmol) and AIBN (0.12 g, 0.06 mmol) were dissolved in DMF (2 mL) in a 25 mL Schlenk tube and reacted for 6 h at 60 °C under nitrogen. Finally, PbP was obtained after precipitated in petroleum ether (Scheme 2B).

Preparation of polyplexes

The polyplexes were formed through electrostatic interaction between PgP and pDNA, or PbP and pDNA. pDNA was diluted to 1 μg/50 μL（containing 3 nmol phosphate groups）in PBS. Polycations were diluted to a certain concentration containing appropriate amino group before added into an equal volume of pDNA and vortexed to get the polyplexes (N/P refers to the molar ratio of amino groups in polycations to the phosphate groups in pDNA). All the suspensions were incubated for 30 min at room temperature before characterization.

Gel permeation chromatography (GPC)

The number-average molecular weight (M_n) and the polydispersities (PDIs) of PVP, PbP and PgP were characterized at 25 °C by gel permeation chromatography (GPC) analysis system with 1 M $NaNO_3$ solution as the eluent at the flow rate of 1 mL min^{-1} and PEO-19K as the calibrate standard.

Particle size and zeta potential measurements

Polyplexes were prepared at the content of 1 μg mL^{-1} of pDNA. The particle size and zeta potential of polyplexes were characterized by Malvern Instruments (Zetasizer 3000HS, Malvern, UK) in PBS buffer (pH 7.4).

Transmission electron microscopy (TEM)

The polyplexes were obtained as described above. All samples were prepared by dipping a drop of polyplexes suspension (nearly 10 μL) onto a Formvar-coated copper grid and dried at room temperature overnight. A Japan JEM-2100F transmission electron microscope was applied here.

Gel retardation assay

10 μL of well incubated polyplexes suspensions were mixed with 2 μL 6× loading buffer (Takara Biotechnology, Dalian, China), then the suspensions were loaded onto 1 wt% agarose gel containing 5 μg mL^{-1} ethidium bromide. Electrophoresis was carried out at a voltage of 120 V for 15 min in 1× TAE running buffer.[7] pDNA retardation was analyzed on image master VDS thermal imaging system (Bio-Rad, Hercules, CA) to show the location of the pDNA.

Measurement of buffering capacity

The buffering capacity of the polymers was measured by acid-base titration. The polymer solutions (10 mL containing 25 mmol amine groups) were titrated with 0.01 M HCl. PEI, PVP and water were titrated as controls. The pH values were recorded at room temperature.

BSA absorption

The stability of the polymers was tested by BSA absorption assay. In brief, 200 μL polymer solutions (1 mg mL^{-1}) mixed with the equal volume of BSA solution (2 mg mL^{-1}). After centrifugation at 13000 r min^{-1} for 15 min, the concentration of BSA in supernatant was calculated through the calibration curve of BSA. The percent of BSA adsorbed on the complexes was calculated through the following equation:

$$q = \frac{(Ci - Cs)V}{m}$$

Ci represents the initial concentration of BSA, and Cs represents the concentration of BSA in the supernatant. V and m represent the ultimate volume of the solution and the weight of the polymer, respectively.

Stability of the polyplexes in the presence of heparin

To compare the stability of the PgP/pDNA, PbP/pDNA and PEI/pDNA polyplexes, the polyplexes containing 1 μg pDNA were incubated with different concentrations of heparin for 2 h. The results were analyzed using agarose gel electrophoresis.

Cell viability

HepG2 cells were seeded in a 96-well plate at a density of 5 × 10^3 cells/well and cultured in complete H-DMEM (90 μL per well) supplemented with 10% FBS, 100 μg mL^{-1} streptomycin and 100 U mL^{-1} penicillin overnight at 37 °C.[36] 10 μL of polyplexes suspensions containing 0.2 μg pDNA at different N/P ratios were added into each well and each ratio was conducted in five parallel groups. After 24 h, the medium was replaced by 100 μL of MTT (0.5 mg mL^{-1} in H-DMEM). After 3 h, the MTT solution was replaced by 150 μL DMSO to ensure full solubilization of the formed formazan crystals. After shaking for 30 s, the absorbance of each well was measured by Infinite M200 (TECAN, Switzerland) at 570 nm, with 630 nm as reference wavelength. The results were expressed as the mean percentage of cell viability relative to untreated cells.

***In vitro* transfection**

HepG2 cells were plated in 24-well plates (0.5 mL，5 × 10^4 cells/well) and incubated in complete H-DMEM overnight. One hour before transfection, the culture medium was replaced by Opti-MEM. After dosing the polyplexes diluted by Opti-MEM, the cells were transfected for 4 h, then replaced by 500 μL complete H-DMEM for additional 44 h prior to analysis.[37] The green fluorescence proteins in the cells were directly observed by an inverted fluorescence microscope (Olympus IX 70, Olympus, Tokyo, Japan) and the transfection efficiency was quantified by flow cytometry (Applied Biosystems, Life Technologies, Carlsbad, CA).

Cellular uptake and cellular distribution of polyplexes

For the cellular uptake process, HepG2 cells were seeded in 24-well plates at the density of 5 × 10^4 cells per well incubated overnight before transfection. Then the cells were transfected with polyplexes containing 1 μg Cy5-Oligo DNA at the N/P ratio of 4:1 for 2 h. Finally, the cells were washed with PBS for three times to remove residual polyplex suspensions, and collected after treated by Trypsin-EDTA, and subsequently

analyzed using an Attune® acoustic focusing cytometer (Applied Biosystems, Life Technologies, Carlsbad, CA).

As to cellular distribution study, 1×10^5 cells were seeded in each of the 35 mm glass dishes one day before transfection. The media were substituted by polyplexes suspensions diluted by Opti-MEM containing 1 μg Cy5-Oligo DNA of each dish. After 4 h incubation, the media were aspirated and substituted by complete H-DMEM. After additional 24 h incubation, each dish was washed with PBS and stained with LysoTracker Green (Invitrogen, Carlsbad, CA) to indicate endosomal/lysosomal organelles. Then the cellular distribution of the polyplexes was observed by confocal laser scanning microscope (CLSM) (LSM 710, Carl Zeiss Microscope Co. Ltd., German) to estimate the intracellular distribution of the polyplexes.[37]

Statistical analysis

Data were expressed as mean ± standard deviations (± S.D.). Statistical analysis was determined using Student's *t*-test and $p < 0.05$ was regarded as statistical significance.

Results and Discussion

Synthesis and characterization of PgP and PbP

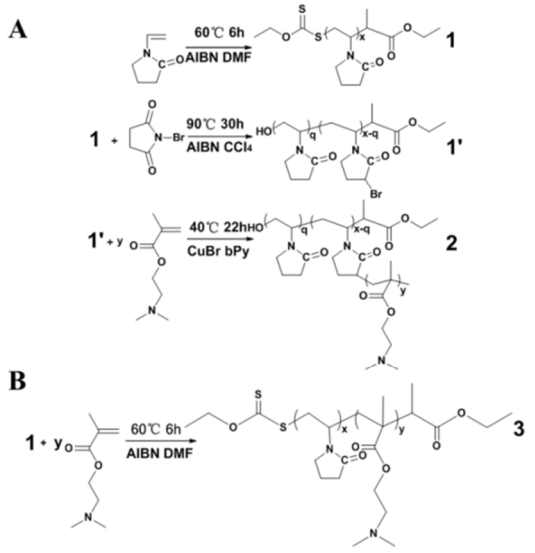

Scheme 2 Synthetic procedures of PgP (A) and PbP (B).

The synthetic procedures of PgP and PbP are shown in Scheme 2. PgP was synthesized by combining application of RAFT and ATRP techniques,[38] while PbP was synthesized by using RAFT technique. Their structures were characterized by ^{1}H NMR and GPC.

The ^{1}H NMR spectra of PVP-CTA, PVP-Br and PgP are shown in Fig. 1A. The characteristic peaks of methylene protons of PVP-CTA appear at 1.9 ppm (indicated by "m") and 3.3 ppm (indicated by "a"). Compared with Fig. 1(A1), the new signals of peaks (indicated by "b'" and "e'") at 2.5 and 4.2 ppm correspond to the H atoms of N-heterocycles replaced by Br atoms, indicating a successful bromination reaction of PVP. The percentage of bromination is 15.99%, calculated by comparing the integral area (S) of H atoms that share common C atoms with Br atoms ("$S_{e'}$", $S_{e'} = 1.41$) to half area of H atoms indicated by "a" ("$S_a/2$", $S_a = 17.64$). In this case, $S_{e'}$ and $S_a/2$ represent the number of brominated N-heterocycles and the number of all the N-heterocycles, respectively. As shown in Fig. 1(A3), the distinctive resonances associated with PDMAEMA can be clearly observed, corresponding to 2.2, 2.6 and 4.0 ppm, which are assigned to the -$N(CH_3)_2$, -$CH_2N<$ and -CH_2-O-, respectively. The peaks of 5.2 ppm and 5.5 ppm represent the -OH of HO-CH_2-CH(N)-, which are formed by the hydrolysis of disulfide bond in CTA. All the results show that PgP was obtained.

Fig. 1B shows the ^{1}H NMR spectra of PVP-CTA and PbP. Besides the specific signals of PVP described above, the characteristic peaks of -$N(CH_3)_2$, -$CH_2N<$ and -CH_2-O- belonging to PbP appear at 2.2, 2.6 and 4.0 ppm, demonstrating the successful synthesis of PbP.

The M_n of PVP-CTA is 5890 calculated from ^{1}H NMR spectra by comparing the integral area of methylene protons at 3.3 ppm (indicated by "a") to the methyl at 1.49 ppm of the CTA as shown in Fig. 1(A1). The degree of polymerization (DP) of DMAEMA for PgP and PbP are 58 and 55, respectively, which is calculated by comparing the area of -CH_2- peak of DMAEMA (indicated by "f") to that of -CH_2- peak of N-heterocycles (indicated by "a") by using the method reported in the references.[9, 38] Consequently, the M_n of PgP and PbP are 15209 and 14792, respectively. In addition, the M_n and PDIs of PVP-CTA, PgP and PbP copolymers were also confirmed by GPC, as shown in Table 1. All the polymers possess narrow PDIs. It can be found that the M_n of the polymers characterized by GPC are lower than those calculated by ^{1}H NMR spectra, which is due to the binding of positive charged PDMAEMA moiety with column packing and PEO-19K calibration used for GPC measurements.[39, 40]

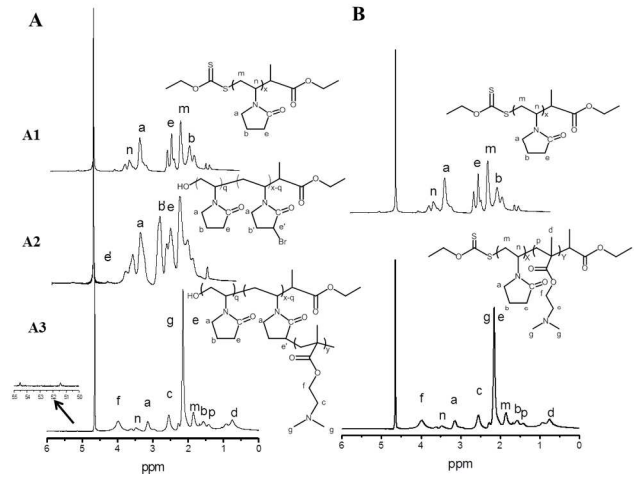

Fig. 1 ^{1}H NMR spectra of PVP-CTA, PgP and PbP. (A) ^{1}H NMR spectra of PVP-CTA (A1), PVP-Br (A2), PgP (A3); (B) ^{1}H NMR spectra of PVP-CTA and PbP.

Table. 1 Characteristics of PVP-CTA, PgP and PbP.

Polymers	Mn^a (g mol^{-1})	Mn^b (g mol^{-1})	Polydispersity^b (M_w/M_n)
PVP-CTA	5890	4760	1.051
PgP	15209	13266	1.064
PbP	14792	11824	1.009

[a] Calculated from ^{1}H NMR. [b] Determined by GPC.

Particle size, zeta potential and morphology

Zeta potential and size are two vital factors of polyplexes for gene delivery.[41-43] As shown in Fig. 2A and Fig. 2B, both PgP and PbP can effectively condense pDNA into 100-200 nm nanoparticles with positive charges when the N/P ratio is above 4:1. With increasing N/P ratios, zeta potentials of PgP/pDNA and PbP/pDNA polyplexes increase from 0 mV to 10 mV and the sizes of them decrease. Compared with PbP/pDNA polyplexes, PgP/pDNA polyplexes show higher zeta potentials and smaller sizes at different N/P ratios. The different zeta potentials of polyplexes may be caused by the different locations of PVP segments. Compared with PgP/pDNA polyplexes, there are more PVP segments on the surrounding of PbP/pDNA polyplexes, which can shield more positive charges. However, PgP has much shorter and stiffer PDMAEMA chains on the side-chains. In this case, the PDMAEMA chains tend to expose on the surrounding of PgP/pDNA polyplexes and reduce the protection of PVP. Therefore, the PgP/pDNA polyplexes exibit higher zeta potentials compared with PbP/pDNA polyplexes. Compared with PbP, PgP has stronger pDNA condensation capacity due to its special architecture, which is the main reason that the sizes of PgP/pDNA polyplexes are smaller than those of PbP/pDNA polyplexes at different N/P ratios.

Their morphologies were further examined by TEM. As shown in Fig. 2C, both PgP/pDNA and PbP/pDNA polyplexes were spherical at the N/P ratio of 4:1. The particle sizes of PgP/pDNA and PbP/pDNA polyplexes are around 180 nm and 220 nm, respectively. The sizes determined by TEM are less than that measured by DLS due to the dehydration of the polyplexes.[8, 44, 45]

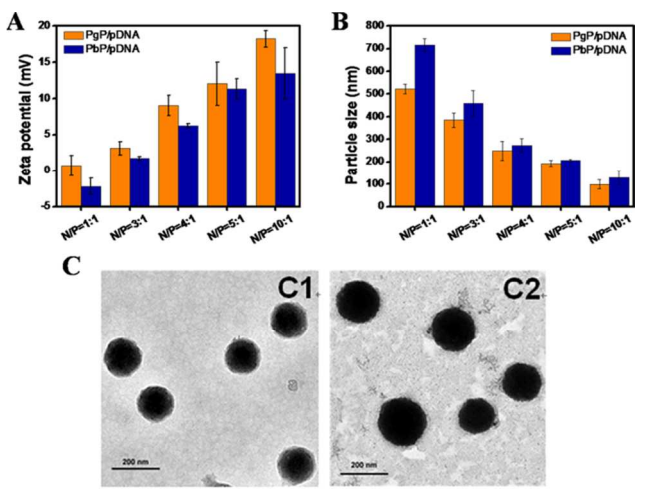

Fig. 2 (A) Zeta potential and (B) size of polyplexes at different ratios of N/P (1:1, 3:1, 4:1, 5:1 and 10:1) (means ± SD, n = 3); (C) TEM images of PgP/pDNA polyplexes (C1) and PbP/pDNA polyplexes (C2) at the N/P ratio of 4:1.

Gel electrophoresis assay

The gel retardation assay was employed to evaluate the pDNA condensation capacity of PgP and PbP. As shown in Fig. 3, PgP and PbP can completely retard pDNA at N/P ratio of 0.8:1 and 2:1 respectively, demonstrating that both PgP and PbP can effectively form polyplexes with pDNA, and PgP shows stronger pDNA condensation capacity than PbP at the same N/P ratio.

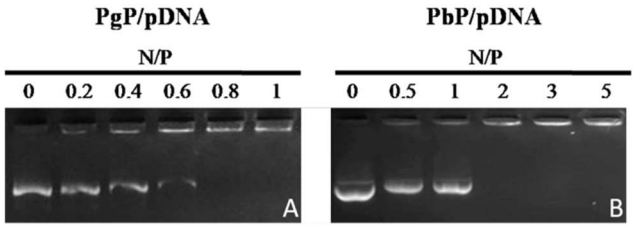

Fig. 3 Gel retardation assay of (A) PgP/pDNA polyplexes and (B) PbP/pDNA polyplexes at different N/P ratios in PBS (pH 7.4).

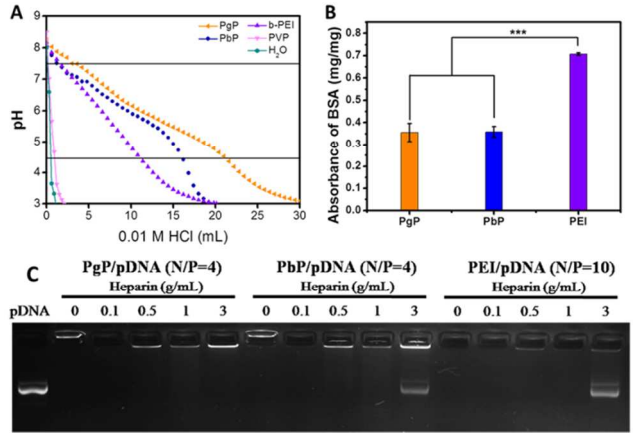

Fig. 4 (A) Acid-base titration profiles of polymers; (B) The BSA absorption of PgP, PbP and PEI; (C) The stability of polyplexes with different concentrations heparin. The N/P ratio of PgP/pDNA and PbP/pDNA polyplexes was 4:1, and the N/P ratio of PEI/pDNA polyplexes was 10:1, ***$p < 0.001$.

Buffering capacity and the stability of the polymers and polyplexes

The buffering capacity of the PgP and PbP were examined through acid-base titration by adding 0.01 M HCl.[46] When water and PVP were titrated, pH decreased dramatically. However, PgP and PbP showed gradual decrease when pH ranged from 7.5 (extracellular pH) to 4.5 (intracellular lysosomal pH).[47] As shown in Fig. 4A, PgP and PbP need 0.174 and 0.148 mmol HCl to drop the pH from 7.5 to 4.5, respectively, while PEI as the positive control need 0.093 mmol, and PVP and water as the negative controls only need 7.3 and 4.0 μmol, respectively. These results indicate that both PgP and PbP have strong buffering ability in the endosomal pH range, and they show better buffering capacity than PEI due to the tertiary amine groups of the PDMAEMA segments.[48] Furthermore, PgP presents better buffering capacity than PbP.

In addition, the stability of the polymers was tested in the presence of excess BSA. As shown in Fig. 4B, PgP and PbP absorb similar amount of BSA, which is much less than PEI, indicating that PgP and PbP composed of PVP and PDMAEMA have better serum resistance ability. It is known that the stability of the polyplexes is crucial for gene delivery. If the polyplexes are unstable, the pDNA of the polyplexes will be easily replaced by the negatively charged macromolecules or cellular components, such as protein, sulfated sugar and nucleic acid, *etc*.[49] In this case, the pDNA will be easily degraded by nuclease and the transfection efficiency will be reduced. Therefore, the stability of the PgP/pDNA, PbP/pDNA and PEI/pDNA polyplexes was subsequently investigated by treating different concentrations of heparin. As shown in Fig. 4C, the stability of the PgP/pDNA polyplexes is stronger than PbP/pDNA polyplexes, which is in accordance with the result that PgP can condense pDNA more effectively compared with PbP.

***In vitro* cytotoxicity and transfection efficiency**

The cytotoxicity of PgP and PbP was evaluated in HepG2 cells through MTT method. As shown in Fig. 5A, PbP/pDNA polyplexes exhibit lower cytotoxicity compared with PgP/pDNA polyplexes, which may result from its lower surface charges.[43, 50] Furthermore, the cytotoxicity of PbP/pDNA polyplexes is comparable to commercial PEI and much lower than Lipofectamine. Although the cytotoxicity of PgP is higher than PEI, it is comparable to Lipofectamine at the N/P ratio of 4:1.

In order to investigate the transfection efficiency of PgP and PbP in HepG2 cells, EGFP-N1 was used as reporter genes and commercial transfection reagents Lipofectamine and PEI (N/P = 10) were used as controls.[51] Fig. 5B shows the green fluorescence proteins of the transfected HepG2 cells at N/P ratios of 3:1, 4:1 and 5:1, respectively. Graft copolymer PgP has much higher gene transfection ability compared with block copolymer PbP, PEI and Lipofectamine. Meanwhile, the transfection efficiency was quantified by flow cytometry (Fig. 5C). The results of flow cytometry are in accordance with the green fluorescence proteins pictures, further demonstrating that the transfection efficiency of PgP is much higher than PbP, especially higher than PEI and Lipofectamine. Combining the results of cell viability and transfection efficiency, the polyplexes at the N/P ratio of 4:1 were selected for further investigation of their gene delivery capacity. In fact, the content of pDNA in polyplexes largely affects the transfection efficiency. The gene transfection of polyplexes with different contents of pDNA was studied to clarify how the content of pDNA affected the transfection efficiency. As shown in Fig. 6, the transfection efficiency of PbP/pDNA polyplexes increases gradually when the pDNA content varies from 0.2 to 1.5 μg/well. When the content of pDNA is 1.2 μg/well, PgP/pDNA polyplexes reach the optimal transfection efficiency about 60%. Notably, the transfection efficiency of PgP/pDNA polyplexes is more than 50% when the pDNA content reaches 0.8 μg/well, indicating that PgP is an effective gene vector.

It should be noted that PgP/pDNA polyplexes present higher transfection efficiency than PbP/pDNA polyplexes, while the cytotoxicity of PbP/pDNA polyplexes is lower than PgP/pDNA polyplexes. It is known that the zeta potential of polyplexes contributed greatly to both transfection efficiency and cytotoxicity. PgP/pDNA polyplexes have more positive surface charges, which benefits cellular uptake.[49] In addition, the buffering capacity of PgP was higher than PbP, which is helpful for endosomal escape. Therefore, the transfection efficiency of PgP was much higher than PbP. The analysis described above was subsequently confirmed by investigating the cellular uptake and endosomal escape behaviors of PgP/pDNA and PbP/pDNA polyplexes.

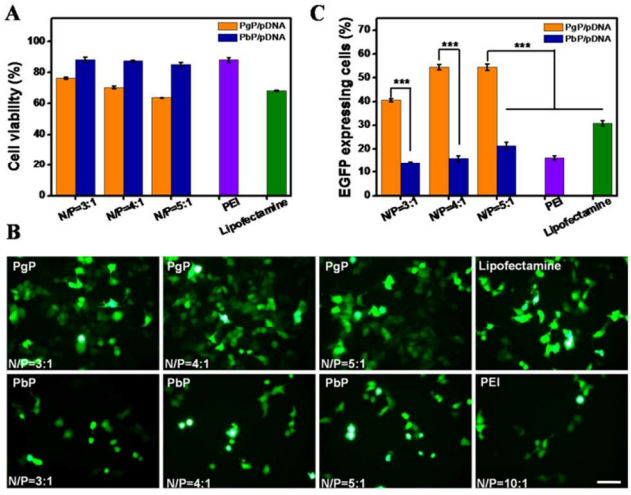

Fig. 5 The cell viability and transfection efficiency of the polyplexes. (A) *In vitro* cell viabilities of HepG2 treated by polyplexes and complexes determined by MTT assay. Experiments were performed in five parallel groups; (B) Fluorescence microscopy images of HepG2 cells transfected with polyplexes. The content of pDNA was 1 μg/well. Bar = 50 μm; (C) The transfection efficiency of polyplexes and complexes quantified by flow cytometry. (means ± SD, n = 3), ***$p < 0.001$.

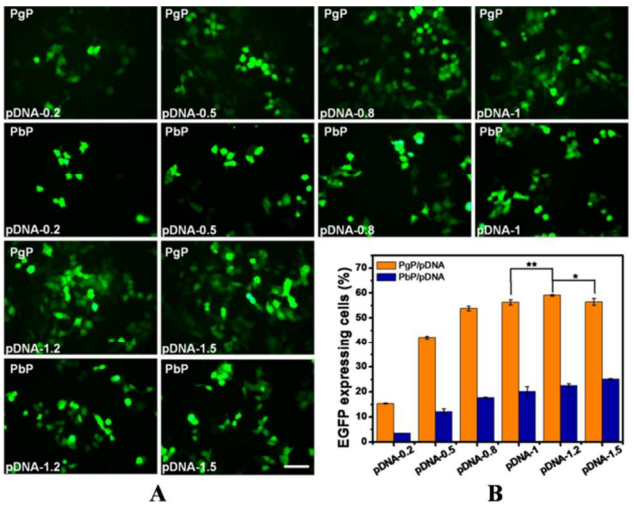

Fig. 6 (A) Fluorescence microscopy images of HepG2 cells transfected with PgP/pDNA polyplexes and PbP/pDNA polyplexes (The content of pDNA varied from 0.2 to 1.5 μg for each well.) Bar = 50 μm; (B) The transfection efficiency of PgP/pDNA polyplexes and PbP/pDNA polyplexes quantified by flow cytometry (means ± SD, n = 3), $*p < 0.05$, $**p < 0.01$.

Internalization of polyplexes

To clearly illustrate the mechanism that the transfection efficiency of PgP is higher than PbP, experiments of cellular uptake and endosomal escape were carried out by using PgP/Cy5-Oligo DNA polyplexes and PbP/Cy5-Oligo DNA polyplexes with Lipofectamine/Cy5-Oligo DNA complexes as control. As shown in Fig. 7A and Fig. 7B, there is no obvious difference of the percentage of fluorescent cells among these polyplexes and complexes. However, the mean fluorescence intensity of PgP/Cy5-Oligo DNA polyplexes is stronger than that of PbP/Cy5-Oligo DNA polyplexes, indicating that the higher zeta potentials of PgP/pDNA polyplexes facilitate its cellular uptake.

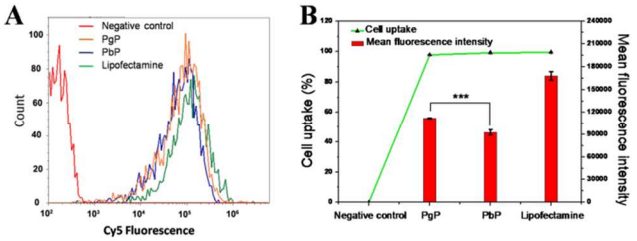

Fig. 7 Cellular uptake of PgP and PbP/Cy5-Oligo DNA polyplexes at N/P ratio of 4:1 in HepG2 cells with Lipofectamine/Cy5-Oligo DNA complexes as positive control. (A) Intracellular fluorescence intensities of PgP/Cy5-Oligo DNA polyplexes, PbP/Cy5-Oligo DNA polyplexes and Lipofectamine/Cy5-Oligo DNA complexes measured by flow cytometry; (B) percentages of cellular uptake and mean fluorescence intensity of polyplexes and complexes measured by flow cytometry. Negative control was the group without any treatment (means ± SD, n = 3), $***p < 0.001$.

Intracellular distribution of polyplexes

It has been confirmed that endosomal escape is a crucial step for gene transfection.[13] The intracellular distributions of these polyplexes were studied by confocal laser scanning microscopy (CLSM). Cy5-Oligo DNA and endosomes/lysosomes stained by Lysotracker green were used to identify the localization of these polyplexes, which displayed yellow when the polyplexes colocalized with endosomes/lysosomes. As shown in Fig. 8A, Compared with PbP/Cy5-Oligo DNA polyplexes, PgP/Cy5-Oligo DNA polyplexes show obviously lower colocalization with endosomes/lysosomes and more released polyplexes (red spot), which is in accordance with the result that the buffering capacity of PgP is stronger than that of PbP. As a comparison, Lipofectamine/Cy5-Oligo DNA complexes and endosomes/lysosomes are also in poor colocalization, indicating that Lipofectamine/Cy5-Oligo DNA complexes also have strong endosomal escape ability. However, most of Lipofectamine/Cy5-Oligo DNA complexes aggregate into particles and most of them localize on the cell surface marked by the red arrows, indicating that the aggregation of Lipofectamine probably results in the decrease of its transfection efficiency.[27] The colocalization ratio of the Cy5-Oligo DNA and Lysotracker Green (endosomes/lysosomes) was also calculated and it was in accordance with the confocal results. Therefore, the high transfection efficiency of PgP originates from the higher cellular uptake efficiency and better endosomal escape compared with PbP.

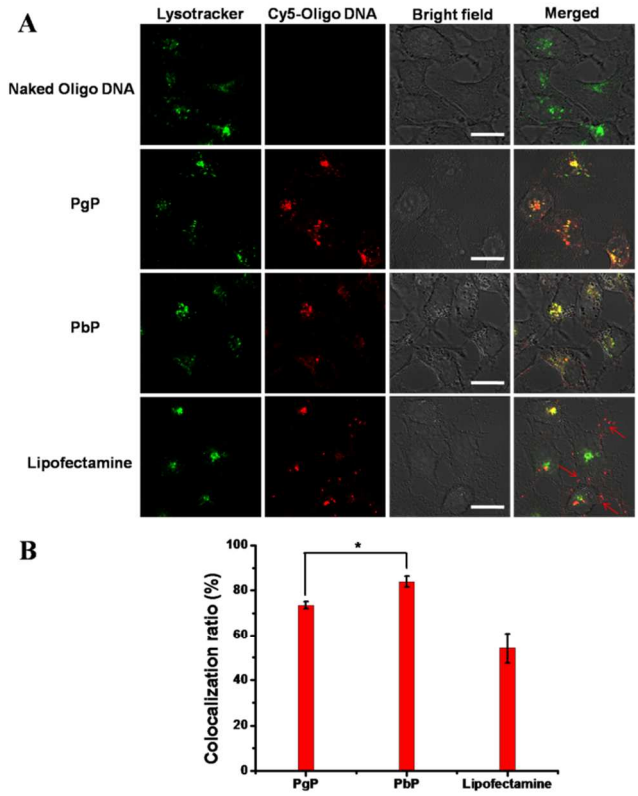

Fig. 8 (A) *In vitro* intracellular distributions of PgP and PbP/Cy5-Oligo DNA polyplexes at N/P ratio of 4:1 in HepG2 cells with Lipofectamine/Cy5-Oligo DNA complexes as positive control. Confocal images were taken after transfection for 24 h. Cy5-Oligo DNA (red) was used. The endosomes and lysosomes were stained with Lysotracker Green (green). Bar = 20 μm; (B) The colocalization ratio of the Cy5-Oligo DNA and Lysotracker Green calculated by Image-Pro Plus 6.0 software, $*p < 0.05$.

Overall, because of the different architecture of PgP and PbP, they showed different properties in gene delivery. PgP can effectively condense pDNA, even at the N/P ratio of 0.8:1, which exhibited higher transfection efficiency than PEI and Lipofectamine. PbP with relatively lower zeta potential (less than 10 mV at the N/P ratio of 4) has lower cytotoxicity compared with PgP. PCL-*g*-PDMAEMA with similar structure as PgP can form core-shell nanoparticles described in the introduction, while PDMAEMA was located at the surface of the nanoparticles. However, the maximum transfection efficiency of PCL-*g*-PDMAEMA was achieved at the N/P ratio of 10,[29] which is bigger than that of PgP (at the N/P ratio of 4) because of the synergistic role of PVP in gene delivery.[52] mPEG-*b*-PDMAEMA and PEG-*a*-PDMAEMA have similar architecture as PbP. All of the three polymers showed no cytotoxicity. However, the gene transfection of mPEG-*b*-PDMAEMA was much lower than that of PDMAEMA.[25] Although the PEG-*a*-PDMAEMA had comparable transfection efficiency with PDMAEMA at the pH of 5.0,[28] the condition was difficult to achieve *in vivo* or *in vitro* (only in lysosome). In addition, the transfection efficiency of PbP was comparable to PEI. Therefore, the study of structural impact of graft and block copolymers based on PVP and PDMAEMA in gene delivery is significant for designing effective gene carriers in the future.

Conclusions

In this study, the properties of PgP and PbP with the same M_n in gene delivery were compared. They had lower BSA absorption and higher buffering capacity compared with PEI. PgP could more effectively condense pDNA. The transfection efficiency of PgP was 40.3%, 52.7% and 52.6% at the N/P ratios of 3:1, 4:1 and 5:1, which was obviously higher than that of PbP, 8.8%, 12% and 15.4%, respectively. The high transfection efficiency of PgP was attributed to the strong cellular uptake and endosome/lysosome escape of the PgP/pDNA polyplexes. PbP had better biocompatibility compared with PgP, and the pDNA of PbP/pDNA polyplexes could more easily separate from PbP. All the results clarified the relationships between structures and properties of the polycations based on PDMAEMA for gene delivery.

Acknowledgements

Authors thank the support of the National Natural Science Foundation of China (31371014, 31100722, 51203111) and Tianjin Natural Science Foundation (13JCYBJC16500). This work was supported by the Chinese Natural Science Foundation Project (30970784, 81171455), a National Distinguished Young Scholars grant (31225009) from the National Natural Science Foundation of China, the National Key Basic Research Program of China (2009CB930200), the Chinese Academy of Sciences (CAS) “Hundred Talents Program” (07165111ZX), the CAS Knowledge Innovation Program and the State High-Tech Development Plan (2012AA020804). The authors also appreciate the support by the "Strategic Priority Research Program" of the Chinese Academy of Sciences (XDA09030301).

Notes and references

[a]*School of Chemical Engineering and Technology, Tianjin University, Tianjin, 300072, China. E-mail:*jinfengxing@tju.edu.cn
[b]*CAS Key Laboratory for Biomedical Effects of Nanomaterials and Nanosafety, National Center for Nanoscience and Technology of China, Zhongguancun, Beijing, 100190, China. E-mail:*liangxj@nanoctr.cn
[c]*College of Material Science and Engineering, Tianjin Polytechnic University, Tianjin, 300387, China. E-mail:*xiaoyans6@163.com
[d]*Collaborative Innovation Center of Chemical Science and Engineering (Tianjin), Tianjin 300072, China.*
†These authors equally contributed to this work.

1. B. Y. Shi, H. Zhang, Z. Y. Shen, J. X. Bi and S. Dai, *Polym. Chem.*, 2013, **4**, 840-850.
2. J. F. Xing, L. D. Deng, S. T. Guo, A. J. Dong and X. J. Liang, *Mini-Rev. Med. Chem.*, 2010, **10**, 126-137.
3. Y. C. Chung, W. Y. Hsieh and T. H. Young, *Biomaterials*, 2010, **31**, 4194-4203.
4. K. Matyjaszewski and N. V. Tsarevsky, *Nat. Chem.*, 2009, **1**, 276-288.
5. T. Albuzat, M. Keil, J. Ellis, C. Alexander and G. Wenz, *J. Mater. Chem.*, 2012, **22**, 8558-8565.
6. L. N. Cui, J. L. Cohen, C. K. Chu, P. R. Wich, P. H. Kierstead and J. M. J. Frechet, *J. Am. Chem. Soc.*, 2012, **134**, 15840-15848.
7. D. Chen, Y. Ping, G. Tang and J. Li, *Soft Matter*, 2010, **6**, 955-964.
8. W. H. Chi, S. Liu, J. X. Yang, R. Y. Wang, H. Q. Ren, H. Zhou, J. T. Chen and T. Y. Guo, *J. Mater. Chem. B.*, 2014, **2**, 5387-5396.
9. X. Y. Yue, W. D. Zhang, J. F. Xing, B. Zhang, L. D. Deng, S. T. Guo, J. Yang, Q. Zhang and A. J. Dong, *Soft Matter*, 2012, **8**, 2252-2260.
10. D. S. Lin, Q. Cheng, Q. Jiang, Y. Y. Huang, Z. Yang, S. C. Han, Y. N. Zhao, S. T. Guo, Z. C. Liang and A. J. Dong, *Nanoscale*, 2013, **5**, 4291-4301.
11. Y. H. Song, T. B. Zhang, X. Y. Song, L. Zhang, C. Q. Zhang, J. F. Xing and X. J. Liang, *J. Mater. Chem. B.*, 2015, **3**, 911-918.
12. D. Z. Zhou, C. X. Li, Y. L. Hu, H. Zhou, J. T. Chen, Z. P. Zhang and T. Y. Guo, *J. Mater. Chem.*, 2012, **22**, 10743-10751.
13. H. C. Kang and Y. H. Bae, *Adv. Funct. Mater.*, 2007, **17**, 1263-1272.
14. M. M. Wang, H. M. Liu, L. Li and Y. Y. Cheng, *Nat. Commun.*, 2014, **5**, 3053 (1-8).
15. H. M. Liu, H. Wang, W. J. Yang and Y. Y. Cheng, *J. Am. Chem. Soc.*, 2012, **134**, 17680-17687.
16. S. K. Samal, M. Dash, S. V. Vlierberghe, D. L. Kaplan, E. Chiellini, C. V. Blitterswijk, L. Moroni and P. Dubruel, *Chem. Soc. Rev.*, 2012, **41**, 7147-7194.
17. L. Han, J. Zhao, X. Zhang, W. P. Cao, X. X. Hu, G. Z. Zou, X. L. Duan and X. J. Liang, *ACS Nano*, 2012, **6**, 7340-7351.
18. H. X. Zeng, H. C. Little, T. N. Tiambeng, G. A. Williams and Z. Guan, *J. Am. Chem. Soc.*, 2013, **135**, 4962-4965.
19. Z. Y. Shen, B. Y. Shi, H. Zhang, J. X. Bi and S. Dai, *Soft Matter*, 2012, **8**, 1385-1394.
20. X. Jiang, M. C. Lok and W. E. Hennink, *Bioconjug. Chem.*, 2007, **18**, 2077-2084.
21. Z. L. Yao and K. C. Tam, *Langmuir*, 2011, **27**, 6668-6673.

22. H. J. Jeon and J. H. Youk, *Macromolecules*, 2010, **43**, 2184-2189.
23. N. S. Ieong, M. Redhead, C. Bosquillon, C. Alexander, M. Kelland and R. K. O'Reilly, *Macromolecules*, 2011, **44**, 886-893.
24. K. Wong, G. B. Sun, X. Q. Zhang, H. Dai, Y. Liu, C. B. He and K. W. Leong, *Bioconjug. Chem.*, 2005, **17**, 152-158.
25. Y. Qiao, Y. Huang, C. Qiu, X. Y. Yue, L. D. Deng, Y. M. Wan, J. F. Xing, C. Y. Zhang, S. H. Yuan, A. J. Dong and J. Q. Xu, *Biomaterials*, 2010, **31**, 115-123.
26. Z. H. Wang, W. B. Li, J. Ma, G. P. Tang, W. T. Yang and F. J. Xu, *Macromolecules*, 2010, **44**, 230-239.
27. S. T. Guo, Y. Y. Huang, W. D. Zhang, W. W. Wang, T. Wei, D. S. Lin, J. F. Xing, L. D. Deng, Q. Du, Z. C. Liang, X. J. Liang and A. J. Dong, *Biomaterials*, 2011, **32**, 4283-4292.
28. S. Lin, F. S. Du, Y. Wang, S. P. Ji, D. H. Liang, L. Yu and Z. C. Li, *Biomacromolecules*, 2007, **9**, 109-115.
29. S. T. Guo, Y. Qiao, W. W. Wang, H. Y. He, L. D. Deng, J. F. Xing, J. Q. Xu, X. J. Liang and A. J. Dong, *J. Mater. Chem.*, 2010, **20**, 6935-6941.
30. I. K. Park, H. L. Jiang, S. E. Cook, M. H. Cho, S. L.. Kim, H. J. Jeong, T. Akaike and C. S. Cho, *Arch. Pharm. Res.*, 2004, **27**, 1284-1289.
31. S. E. Cook, I. K. Park, E. M. Kim, H. J. Jeong, T. G. Park, Y. J. Choi, T. Akaike and C. S. Cho, *J. Control. Release.*, 2005, **105**, 151-163.
32. F. A. Plamper, H. Becker, M. Lanzendörfer, M. Patel, A. Wittemann, M. Ballauff and A. H. E. Müller, *Macromol. Chem. Phys.*, 2005, **206**, 1813-1825.
33. M. Semsarilar, E. R. Jones, A. Blanazs and S. P. Armes, *Adv. Mater.*, 2012, **24**, 3378-3382.
34. M. J. Manganiello, C. Cheng, A. J. Convertine, J. D. Bryers and P. S. Stayton, *Biomaterials*, 2012, **33**, 2301-2309.
35. Z. H. Wang, Y. Zhu, M. Y. Chai, W. T. Yang and F. J. Xu, *Biomaterials*, 2012, **33**, 1873-1883.
36. H. Gao, X. Y. Lu, Y. A. Ma, Y. W. Yang, J. F. Li, G. L. Wu, Y. N. Wang, Y. N. Fan and J. B. Ma, *Soft Matter*, 2011, **7**, 9239-9247.
37. J. L. Chen, X. Y. Sun, Z. W. Yu, J. Q. Gao and W. Q. Liang, *Int. J. Pharm.*, 2012, **422**, 510-515.
38. B. Zhang, L. D. Deng, J. F. Xing, J. Yang and A. J. Dong, *J. Biomater. Sci-Polym. Ed.*, 2013, **24**, 45-60.
39. W. L. Zhang, J. L. He, Z. Liu, P. H. Ni and X. L. Zhu, *J. Polym. Sci. Part A: Polym. Chem.*, 2010, **48**, 1079-1091.
40. B. C. Anderson, S. M. Cox, P. D. Bloom, V. V. Sheares and S. K. Mallapragada, *Macromolecules*, 2003, **36**, 1670-1676.
41. A. F. Radovic-Moreno, T. K. Lu, V. A. Puscasu, C. J. Yoon, R. Langer and O. C. Farokhzad, *ACS Nano*, 2012, **6**, 4279-4287.
42. B. Mahltig, J. F. Gohy, S. Antoun, R. Jerome and M. Stamm, *Colloid Polym. Sci.*, 2002, **280**, 495-502.
43. S. Mansouri, Y. Cuie, F. Winnik, Q. Shi, P. Lavigne, M. Benderdour, E. Beaumont and J. C. Fernandes, *Biomaterials*, 2006, **27**, 2060-2065.
44. Y. L. Luo, X. Y. Yao, J. F. Yuan, T. Ding and Q. Y. Gao, *Colloids. Surf. B.,* 2009, **68**, 218-224.
45. V. A. Ernesto, N. R. Rafael, F. V. Juan , H. Ping and M. S. Javier, *Eur. Biophys. J. Biophy.*, 2011, **40**, 835-842.
46. H. Koo, G. W. Jin, H. Kang, Y. Lee, K. Nam, C. Z. Bai, J. S. Park, *Biomaterials*, 2010, **31**, 988-998.
47. Y. M. Liu, T. M. Reineke, *Bioconjug. Chem.*, 2007, **18**, 19-30.
48. S. C. Han, H. Y. Wan, D. S. Lin, S. T. Guo, H. X. Dong, J. H. Zhang, L. D. Deng, R. M. Liu, H. Tang and A. J. Dong, *Acta. Biomater*, 2014, **10**, 670-679.
49. M. H. Ki, J. E. Kim, Y. N. Lee, S. M. Noh, S. W. An, H. J. Cho and D. D. Kim, *Pharm. Res.*, 2014, **31**, 3323-3334.
50. P. Pierrat, R. Wang, D. Kereselidze, M. Lux, P. Didier, A. Kichler, F. Pons and L. Lebeau, *Biomaterials*, 2015, **51**, 290-302.
51. M. C. Deshpande, M. C. Davies, M. C. Garnett, P. M. Williams, D. Armitage, L. Bailey, M. Vamvakaki, S. P. Armes and S. Stolnik, *J. Control. Release.*, 2004, **97**, 143-156.
52. X. J. Chang, Z. X. Wang, S. Quan, Y. C. Xu, Z. X. Jiang and L. Shao, *Appl. Surf. Sci*.,2014, **316**, 537-548.

Table of contents

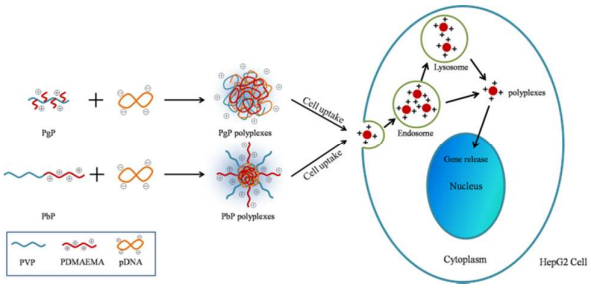

The characteristics of graft copolymer and block copolymer based on PVP and PDMAEMA with equal molecular weight of PDMAEMA in pDNA compaction, polyplexes stability, cytotoxicity, transfection efficiency, internalization and intracellular distribution were systematically investigated.